

# Laser induced modification of alkali borate glasses

Ben Franta, Landon Tweeton, Steve Feller & Mario Affatigato\*

Physics Department, Coe College, 1220 First Av. NE, Cedar Rapids, IA 52402, USA

Manuscript received 21 August 2008

Revised version received 11 February 2009

Accepted 19 August 2009

We report on the effects of 785 nm light irradiation at 84 and 160 mW on copper-doped alkali borate glasses. Glasses of the chemical formula  $y(\text{CuO}) \cdot (1-y)[x(\text{Z}_2\text{O}) \cdot (1-x)(\text{B}_2\text{O}_3)]$  were made, with  $y=0.05$ ,  $0.1 < x < 0.5$ , and Z representing either Li or Cs. Modification of the surface, including crystallisation, was measured as a function of laser power and sample composition. Laser drawn surface patterning and spheroidisation were also performed. Scanning electron microscopy, atomic force microscopy, micro-Raman spectroscopy, and x-ray fluorescence spectroscopy were used to characterise the changes induced by the laser light.

## 1. Introduction

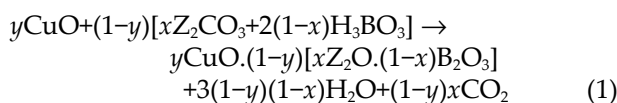
The effects of laser irradiation on glasses has been studied for several years. Borates, in particular, have been crystallised<sup>(1)</sup> and selectively patterned<sup>(2)</sup> through laser exposure, and numerous glass families have been examined, including GeSe<sub>2</sub>, zinc tellurite,<sup>(3)</sup> and PbI<sub>2</sub>-doped lead germanate glasses.<sup>(4)</sup> This paper follows a similar study on vanadate glasses<sup>(5)</sup> which suggested a thermally driven mechanism for the formation of various crystal forms observed on the surface.

Here, we report on our studies of the laser irradiation of copper-doped alkali borate glasses, which can be modified with 785 nm light at relatively low (84–160 mW) powers. Observed changes due to irradiation include topographical alterations and crystallisation, surface patterning and spheroidisation of particles, and the removal of surface crystals which had formed spontaneously on hygroscopic samples when left in air.

## 2. Experimental procedure

### 2.1 Glassmaking procedure

Glasses were prepared according to the following reaction



where Z represents either Li or Cs. The starting materials for the glasses were copper (II) oxide (Alfa Products, 99.0%), lithium carbonate (Aldrich, 99%+), caesium carbonate (Sigma-Aldrich, 99%), and boric acid (Sigma-Aldrich, 99.99%). The value of  $y$  was held constant at 0.05 (5 mol%) for all samples in order to increase absorption at the laser wavelength (785 nm), and  $x$  was varied from 0.1 to 0.5. The powders

were thoroughly mixed in a platinum crucible and heated to 1000°C in an electric muffle furnace. After 10 min the melt was removed from the furnace, allowed to cool, and a weight measurement was taken to ensure composition. The sample was then placed back in the furnace for a further 10 min at 1000°C, and subsequently cooled by splat quenching between two stainless steel plates. The cooling rate was approximately 10000°C/s. Sample thickness was approximately 1.5 mm. Water sensitive samples were stored in a bell jar desiccator.

Crystals of compositions Li<sub>2</sub>O.B<sub>2</sub>O<sub>3</sub>, Cs<sub>2</sub>O.B<sub>2</sub>O<sub>3</sub>, Cs<sub>2</sub>O.2B<sub>2</sub>O<sub>3</sub>, and Cs<sub>2</sub>O.3B<sub>2</sub>O<sub>3</sub> were fabricated through a process of devitrification. Appropriate amounts of chemical powder were mixed and heated as above. Afterwards, the samples were placed in an annealing furnace at 80°C above the glass transition temperature,  $T_g$ , and allowed to devitrify for at least 16 h.

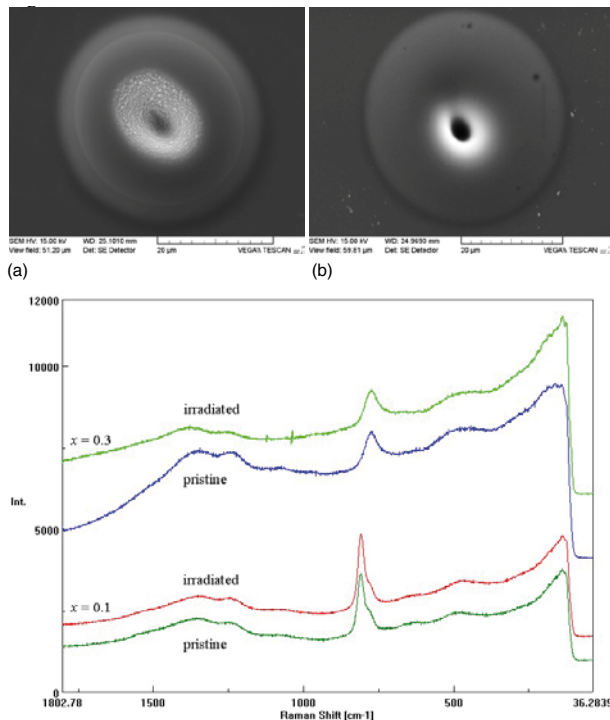
### 2.2. Laser irradiation procedure

The Raman system used for the laser irradiation and analysis was a JASCO NRS-3100 micro-Raman spectrophotometer. A Torsana Starbright 785 nm SLM diode laser with a spot diameter size of 2 μm was used to irradiate the sample at 84 mW and 160 mW for durations ranging from 5 to 40 s. Spectra were then acquired with the laser power attenuated to 16 mW at various sites within the resulting affected area; this power level was not sufficient to cause surface alterations. Changes in the Raman spectrum as a function of distance from the centre of the irradiation site were identified.

### 2.3. Scanning electron microscopy and x-ray fluorescence spectroscopy

A Tescan Instruments Vega-II Scanning Electron Microscope (SEM) and an Oxford Instruments Inca PentaFET were used for imaging and chemical analy-

\* Author to whom correspondence should be addressed. Email maffatig@coe.edu



(c) Figure 1. (a) SEM image of lithium borate sample with  $x=0.1$ , irradiated at 160 mW for 30 s; (b) Lithium borate sample with  $x=0.3$ , irradiated at 160 mW for 30 s. (c) Raman spectra of these samples, pristine and irradiated, indicating that the affected regions are still amorphous

sis. Samples were gold coated with a sputter coater prior to SEM analysis. Images were taken using a side electron detector and with column potentials of 15 and 30 kV. Elemental population spectra were quantitatively optimised using the copper signal of the sample, and relative abundances were calculated using a boron-to-oxygen ratio normalisation. To ensure consistency, multiple readings of areas exhibiting similar surface characteristics were performed and then averaged.

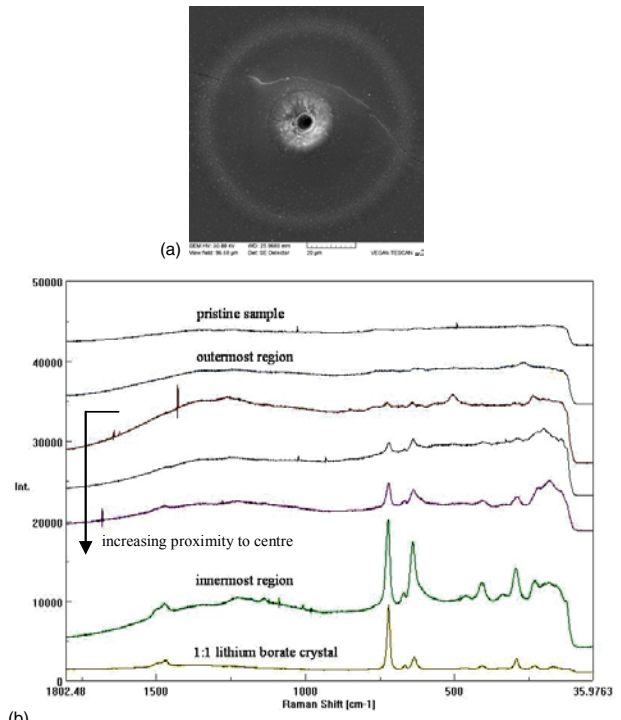
### 2.4. Atomic force microscopy

A Veeco Multimode Atomic Force Microscope (AFM) was used to analyse the surface morphology of caesium borate glasses in which lines had been drawn with laser irradiation. The AFM tapping mode was used, with the piezoelectric scanner mapping out a 60×60 μm area with a maximum z-range of 5.1 μm. No post-acquisition filtering was carried out.

## 3. Results

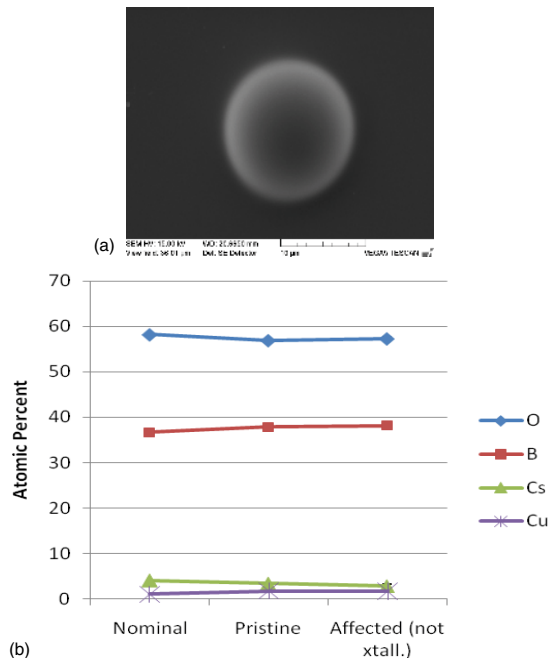
### 3.1. Crystallisation of sample surface

Figure 1 shows Raman spectra and scanning electron micrographs of lithium borate samples with  $x$  values of 0.1 and 0.3, after exposure to 160 mW laser light. Figure 2 shows the same for the lithium metaborate composition ( $x=0.5$ ), and indicates an increasing level



(b) Figure 2. (a) SEM image of a lithium borate sample with  $x=0.5$ , irradiated at 160 mW for 30 s. Note the crystalline region proximal to the centre. (b) Raman spectra, showing increasing crystallisation towards the centre of the irradiation site

of laser induced crystallisation proximal to the centre of the irradiation site (Raman spatial resolution is approximately 2 μm). X-ray chemical analysis was



(b) Figure 3. (a) Caesium borate sample with  $x=0.1$ , irradiated at 160 mW for 30 s; (b) x-ray fluorescence chemical analysis, showing homogeneous composition throughout the region of laser exposure. Interpolating lines serve as a guide to the eye

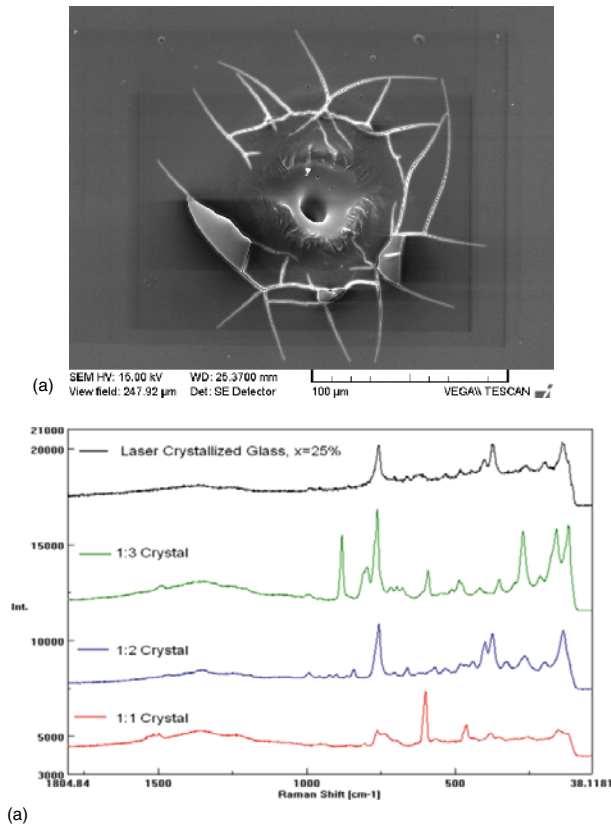


Figure 4. (a) Caesium borate with  $x=0.25$ , irradiated at 160 mW for 40 s; (b) Raman spectra, showing a comparison of the crystallised inner ridge formed under laser exposure to the 1:3, 1:2, and 1:1 caesium borate crystals. Note the agreement between the irradiated glass and the 1:2 caesium borate crystal

not performed with these samples as the technique is not well suited to making accurate measurements of lithium.

As shown in Figure 3, low caesium content glasses ( $x=0.1$ ) displayed limited topographical changes, forming a spot approximately 15  $\mu\text{m}$  in diameter. Analysis with Raman spectroscopy showed this area to remain structurally amorphous. Mid-range compositions ( $x=0.25$ ) exhibited significant changes in response to the 785 nm irradiation, often including the formation of a crystalline ridge surrounding the centre of the affected area, as shown in Figure 4. Figure 5 displays data pertaining to the  $x=0.3$  composition, which also exhibited a region of crystallisation. The Raman spectrum of this area (Figure 5(b)) compares favourably with that of the prepared  $\text{Cs}_2\text{O}\cdot 2\text{B}_2\text{O}_3$  crystal. Unlike lithium, caesium levels can be accurately measured using x-ray fluorescence spectroscopy, so chemical analyses were carried out on various regions surrounding each irradiation site. Preliminary results were inconclusive, but indicated stable chemical populations throughout irradiated areas which remained amorphous, and suggested slight changes in the caesium content of crystalline areas. We are in the process of refining these measurements.

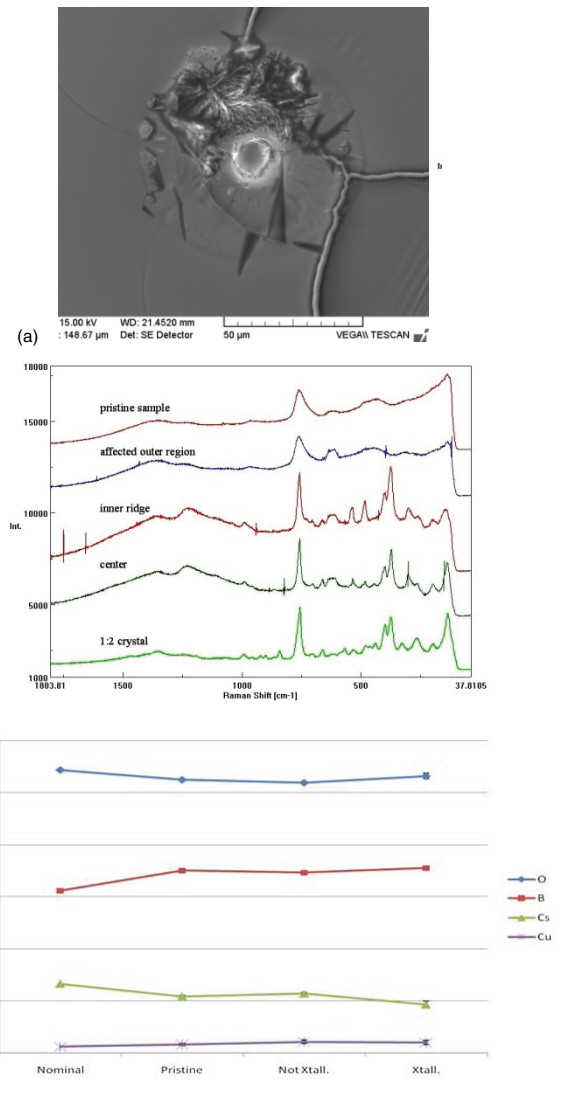


Figure 5. (a) SEM image of caesium borate with  $x=0.3$ , irradiated at 160 mW for 30 s; (b) Raman spectra of various regions, showing the presence of  $\text{Cs}_2\text{O}\cdot 2\text{B}_2\text{O}_3$  crystal; (c) chemical analysis of various regions. Interpolating lines serve as a guide to the eye

Caesium borate glasses of composition  $x=0.4$  and  $0.5$  were water sensitive and crystallised spontaneously when exposed to the atmosphere. Laser exposure had the effect of removing this crystallisation, as shown in Figure 6. Raman data demonstrated that the sample surface was amorphous during irradiation. The Raman spectrum of the crystals themselves could not be acquired, as even modest laser energies caused them to disappear.

### 3.2. Surface patterning

Caesium borate glasses with  $x=0.25$  were exposed to 785 nm laser irradiation at 84 mW, which caused surface modification but was insufficient to crystallise the sample. During irradiation, the sample position was manipulated to result in a pattern of parallel

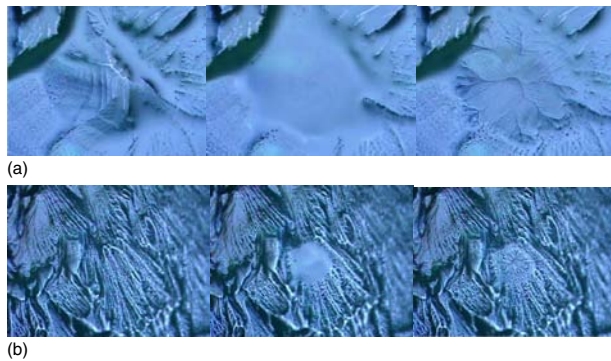


Figure 6. Optical micrographs of caesium borates with  $x=0.5$ , showing dispersion of surface crystals under laser irradiation and subsequent reformation (all images are  $500\ \mu\text{m}$  across). (a) left: before irradiation; centre: immediately after irradiation at  $160\ \text{mW}$ ; right:  $10\ \text{s}$  after irradiation. (b) left: before irradiation; centre: immediately after irradiation at  $84\ \text{mW}$ ; right:  $5\ \text{s}$  after irradiation

lines, as shown in Figure 7. Figure 7(b) shows a cross-sectional analysis of the surface morphology of the sample, indicating a nearly sinusoidal behaviour. The imprinted lines are approximately  $375\ \text{nm}$  high and have a period of  $25\ \mu\text{m}$ .

### 3.3. Spheroidisation

Caesium borate glass with  $x=0.1$  was ground into a fine powder with a mortar and pestle. The powder was placed on a microscope glass slide and individual particles were irradiated at  $16\ \text{mW}$ , resulting in an immediate spheroidisation of the grains. The spheres, approximately  $40\ \mu\text{m}$  in diameter, were adhered to a carbon disk and gold coated before SEM imaging, as shown in Figure 8. The results were nearly spherical; one flat portion remained where the glass particle was in contact with the microscope slide.

### 3.4. Area of effect

Figure 9 shows a caesium borate glass ( $x=0.3$ ) after the gold coating needed for SEM analysis had begun to flake off, an occurrence commonly observed over a period of days with both lithium and caesium borate glasses. Although laser irradiation produced an initial area of visible effect less than  $100\ \mu\text{m}$  in diameter, the gold coating is preserved around the exposure site to a radius of  $1\ \text{mm}$ . This suggests that areas which are far away from the irradiation site may still be affected, perhaps thermally.

## 4. Discussion

### 4.1. Crystallisation of sample surface

Results from Raman spectroscopy and scanning electron microscopy point to significantly different irradiation effects, which are dependent upon the alkali content of the glass. Exposure of lithium bo-

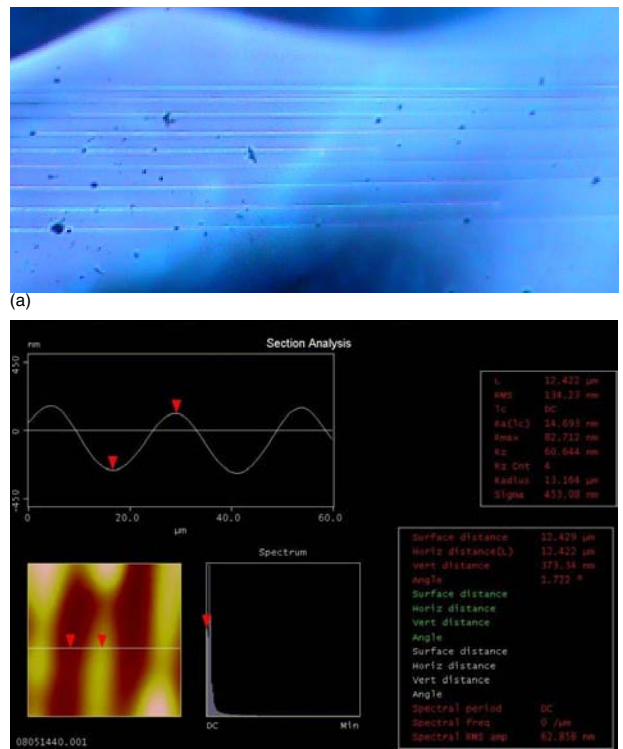


Figure 7. (a) Optical micrograph of caesium borate with  $x=0.25$ , irradiated with  $785\ \text{nm}$  laser light at  $84\ \text{mW}$  focused through a  $100\times$  lens. Image acquired under  $5\times$  magnification with writing rates of approximately  $1\text{--}2\ \text{mm/s}$ . (b) Computer screenshot of an AFM sectional analysis of the striations, showing a mound-like morphology

rate samples with  $x$  values of  $0.1$  and  $0.3$  to  $160\ \text{mW}$  laser light produced topographical changes, but, as evidenced by Raman spectroscopy, did not produce structural changes. This is in agreement with the thermal behaviour: the glass transition temperature increases<sup>(6)</sup> from  $343^\circ\text{C}$  to  $496^\circ\text{C}$  over the range in  $x$  from  $0.1$  to  $0.3$  for undoped lithium borates. The lithium metaborate composition, on the other hand,

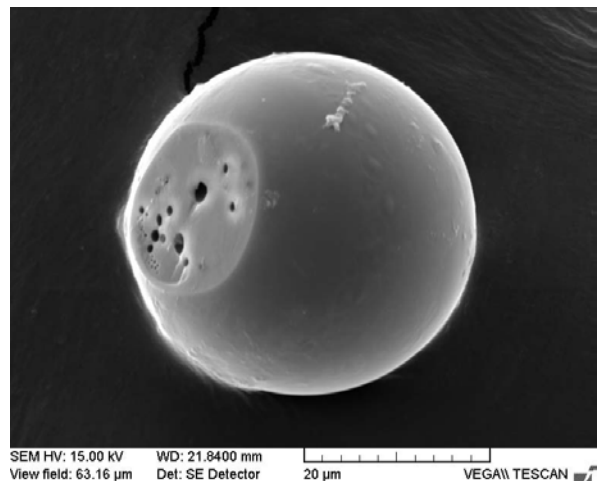


Figure 8. Sphere made from an irradiated powder of  $x=0.1$  caesium borate glass. The flat portion indicates the area which was the bottom of the sphere as it formed



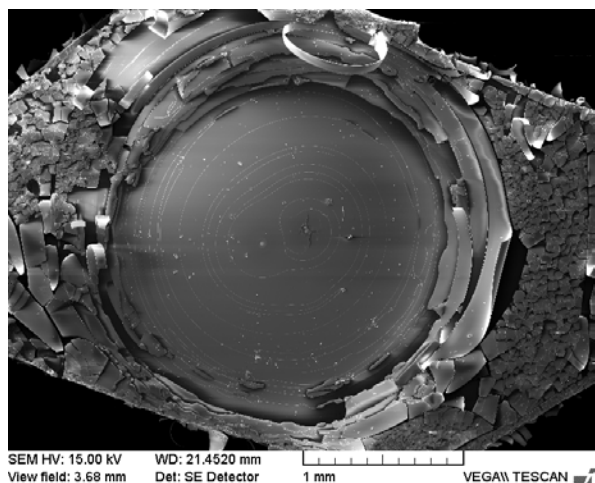


Figure 9. Caesium borate glass with  $x=0.3$ , two days after irradiation for 30 s at 160 mW. Original area of effect was less than 100  $\mu\text{m}$  in diameter. As the gold film required for SEM analysis peels from the surface, an area of effect due to laser exposure is observed which is 1 mm in diameter

did show evidence of crystallisation at the irradiation site (Figure 2). As expected, the Raman signal of this laser induced crystal was seen to match that of a laboratory prepared  $\text{Li}_2\text{O}\cdot\text{B}_2\text{O}_3$  crystal. Exposure duration was not observed to significantly affect the size or overall response of the modified area; however, the affected area of the lithium metaborate composition was significantly larger than that of the other two. A dimple or hole is often observed at the centre of the irradiation site (e.g. Figures 1, 2, and 4), and is likely to be a result of mass transfer due to laser exposure. This hole does not extend completely through the sample.

The response of caesium borate glasses to laser irradiation was, again, dependent upon composition. Low caesium compositions ( $x=0.1$ ; Figure 3) remained amorphous, while midrange compositions ( $x=0.25$  and  $x=0.3$ ; Figures 4 and 5) underwent crystallisation. This was somewhat unexpected, as the glass transition temperature actually increases<sup>(6)</sup> for the midrange composition, reaching 430°C for pure (i.e.  $y=0$ ) caesium borate glasses. A Raman comparison with three caesium borate crystals (with  $x=0.25$ , 0.33, and 0.50) suggested that the laser induced crystalline area was composed of  $x=0.33$  caesium borate crystal (see Figures 4(b) and 5(b)). This indicates that the crystalline areas are caesium enriched during irradiation, and that compositional proximity to the crystal stoichiometry was a key factor in the crystallisation.

For high caesium compositions ( $x=0.4$  and  $x=0.5$ ), laser exposure resulted in the immediate vitrification of crystals which formed due to the hygroscopic nature of the glasses. The absence of irradiation allowed crystal regrowth to occur over a short period ( $\sim 10$  s; see Figure 6). Because these crystals are most likely formed as a result of hydrolysis, we expect their dispersion by laser irradiation to be caused by

a heating and drying of the surface – essentially a thermal phenomenon.

#### 4.2. Surface patterning

Analysis of the laser drawn lines with atomic force microscopy (Figure 7(b)) indicated that the patterning is formed when the sample material expands under laser exposure, resulting in a continuous, shallow mound.

#### 4.3. Spheroidisation

Figure 8 displays a single vitreous grain ( $x=0.1$  caesium borate) spheroidised by laser irradiation. Numerous microvoids can be seen extending into the interior of the sphere. Again, the spheroidisation process appears to be thermally driven in nature, a result of the glassy grain being heated beyond its glass transition temperature. The sphere remained amorphous after irradiation, indicating the crystallisation temperature,  $T_v$ , had not been reached.

#### 4.4. Area of effect

In general, the area of visible surface change due to laser irradiation tends to become greater as alkali content increases. For instance, the  $x=0.1$  caesium borate exhibited an area of effect of approximately 15  $\mu\text{m}$  in diameter, while the  $x=0.5$  sample of the same series showed an affected area which had a diameter of greater than 500  $\mu\text{m}$ . Although visible changes may not be apparent outside these areas, Figure 9 suggests that larger regions of the sample may be affected, nevertheless. For instance, it is possible that, due to these hygroscopic nature of the glasses, a layer of moisture which may normally form on the glass surface evaporated near the irradiation site, allowing the gold coating to bond more strongly to the surface in that area.

### 5. Conclusions

We have investigated changes in the morphology of copper-doped alkali borate glass upon irradiation with 785 nm laser light. Low alkali content glasses were visibly altered, but not crystallised, at the site of exposure. Higher alkali content glasses showed further surface alterations, such as the formation of crystals. Chemical analysis results indicated that compositional changes were taking place, particularly in regions which appeared to be crystalline. The  $x=0.4$  and  $x=0.5$  compositions of caesium borate exhibited spontaneous surface crystallisation when exposed to air. Laser exposure resulted in vitrification of the site, which then quickly recrystallised in the absence of irradiation.

Other laser induced modifications were produced as well, including the formation of surface striations.

AFM analysis of this surface patterning showed the laser drawn lines to be formed by an expansion of the irradiated material. The surface was shown to be morphologically sinusoidal. The irradiation of small grains was also carried out, resulting in the fabrication of glassy spheres approximately 40  $\mu\text{m}$  in diameter.

Interactions between the glass sample and a gold coating indicated an area of effect from laser exposure which was much greater than the visibly altered site. This supports the suggestion that the laser induced effects are essentially thermal in nature.

### Acknowledgments

We would like to acknowledge the financial support of the US National Science Foundation under grants DMR-MRI-0722682, DMR-MRI-0420539, DMR-MRI-0320861, and DMR-0502051. The authors

would also like to thank Coe College for its continued support and Dr Norimasa Umesaki and the other organisers of the Sixth International Conference on Borate Glasses, Crystals and Melts.

### References

1. Kamitsos, E. I., Karakassides, M. A., Patsis, A. P. & Chryssikos, G. D. *J. Non Cryst. Solids*, 1990, **116**, 115.
2. Honma, T., Benino, Y., Fujiwara, T., Sato, R. & Komatsu, T. *J. Non Cryst. Solids*, 2004, **345&346**, 127.
3. Haro, E., Xu, Z. S., Morhange, J. F., Balkanski, M., Espinosa, G. P. & Phillips, J. C. *Phys. Rev. B*, 1985, **32**, 969.
4. Goutaland, F., Mortier, F., Capoen, B., Turrell, S., Bouazaoui, M., Boukenter, A. & Ouerdane, Y. *Opt. Mater.*, 2006, **28**, 1276.
5. Franta, B., Williams, T., Faris, C., Feller, S. & Affatigato, M. *Phys. Chem. Glasses: Eur. J. Glass Sci. Technol. B*, 2007, **48**, 357.
6. Feller, S. A., Kottke, J., Welter, J., Nijhawan, S., Boekenhauer, R., Zhang, H., Feil, D., Parameswar, C., Budhwani, K., Affatigato, M., Bhatnagar, A., Bhasin, G., Bhowmik, S., Mackenzie, J., Royle, M., Kambeyanda, S., Pandikuthira, P. & Sharma, M. In: *Borate glasses, crystals and melts*, Eds. A. C. Wright, S. A. Feller & A. C. Hannon, Society of Glass technology, Sheffield, 1997, p. 246.